NIST NSRDS 64

NIST Electron Elastic-Scattering Cross-Section Database

Version 4.0
User's Guide

A. Jablonski
F. Salvat
C. J. Powell

NIST
National Institute of
Standards and Technology
U.S. Department of Commerce

NIST NSRDS 64

NIST Electron Elastic-Scattering Cross-Section Database

Version 4.0
User's Guide

A. Jablonski
Polish Academy of Sciences

F. Salvat
Universitat de Barcelona, Barcelona

C. J. Powell
Materials Measurement Science Division
Material Measurement Laboratory
National Institute of Standards and Technology

September 2016

U.S. Department of Commerce
Penny Pritzker, Secretary

National Institute of Standards and Technology
Willie May, Under Secretary of Commerce for Standards and Technology and Director

TABLE OF CONTENTS

1. Introduction

Theoretical description of electron transport in solids is important in radiation physics, electron lithography, electron-probe microanalysis, analytical electron microscopy, and surface analysis by Auger electron spectroscopy (AES) and X-ray photoelectron spectroscopy (XPS). In these and other applications, the trajectories of electrons in a solid are generally modified by single and multiple elastic-scattering events. An evaluation of the effects of elastic scattering on the process of interest requires knowledge of the cross sections for electron elastic scattering by the constituent atoms of the particular solid. Although calculated and measured electron elastic-scattering cross sections are available in the literature for selected elements and a limited number of electron energies, this information is incomplete and insufficient for general use.

NIST released Version 1.0 of the Elastic-Electron-Scattering Cross-Section Database (SRD 64) in 1996. This version provided differential and total elastic-scattering cross sections for elements with atomic numbers from 1 to 96 and for electron energies between 50 eV and 9999 eV in steps of 1 eV. These cross sections were calculated using the Thomas-Fermi-Dirac potential to describe the interaction between an electron and an atom, and using both relativistic and non-relativistic models. This version was designed for analyses of the transport of signal electrons in AES and XPS although it could, of course, be used for other applications.

Version 2.0 of the database was released in 2000. In this version, the upper electron-energy limit was extended to 20 keV, and phase shifts and transport cross sections were also provided. The elastic-scattering cross sections, phase shifts, and transport cross sections, however, were obtained only with a relativistic model because this was believed to be more reliable than the non-relativistic model.

Version 3.0 of the database was released in 2002, and contained two major changes. First, the differential elastic-scattering cross sections, total elastic-scattering cross sections, phase shifts, and transport cross sections were calculated from a relativistic Dirac partial-wave analysis in which the potentials were obtained from Dirac-Hartree-Fock electron densities computed self-consistently for free atoms. This potential is believed to be more reliable than the Thomas-Fermi-Dirac potential used previously [1]. Differences in elastic-scattering cross sections and transport cross sections resulting from this change of potential were described in a review article [1].

In addition, it is possible in Version 3.0 to create and/or print files illustrating variation of differential elastic-scattering cross sections versus scattering angle for one or more elements or for one or more energies. Some of the database screens were redesigned as a result of the increase in the upper electron-energy limit to 300 keV.

Version 3.1 of the database, issued in August, 2003, contains two corrections to Version 3.0. First, a numerical mistake was found in the calculation of differential cross sections for a small number of elements and energies (e.g., F at 300 eV). Second, the routine used for interpolations between differential cross sections at certain scattering angles was found to be inadequate in the vicinity of deep minima in the differential cross sections (e.g., Cu at 319 eV). The libraries of cross-section data and the software have been revised to correct these problems.

Version 3.2 of the database was issued in December, 2010. The installation program for Version 3.2 was changed so that it would operate on newer versions of the Windows operating system. There were no changes or additions to the data in the database although a new About box was added to the main menu. This box shows two references, a 2004 critical review [1] and a 2005 review [2], that discuss evaluations of the compiled data, methods of determination, and uncertainty.

Version 3.2 of the Electron Elastic-Scattering Cross-Section Database had the following capabilities:
- Graphical display of differential elastic-scattering cross sections in different coordinate systems
- Graphical display of the dependence of transport cross sections on electron energy
- Display of numerical values of differential elastic-scattering cross sections, total elastic-scattering cross sections, and transport cross sections
- Creation of files containing differential elastic-scattering cross sections for specified elements, energies and coordinates
- Creation of files containing plots of differential elastic-scattering cross sections versus scattering angle for one or more elements or for one or more electron energies
- Creation of files containing phase shifts for specified elements and for energies up to 20,000 eV
- Creation of files containing transport cross sections for specified elements and energies
- Creation of random number generators providing the polar scattering angles to be used in Monte Carlo simulations of electron transport in solids; and
- Runs of the random number generators

Version 4.0 of the database was released in August, 2016. The database has been redesigned to operate in a user's browser rather than as an installed database on a personal computer with the Windows operating system. All screens have been redesigned. The database now provides differential elastic-scattering cross section and transport cross sections, as in previous versions. Graphical displays of these cross sections are available as before. Three types of data files can be downloaded:

- Javascript object notation (JSON) files
- Comma separated variable (CSV) files that can be opened by spreadsheet software
- Text files that can be easily read by user programs.

Phase Shifts are not provided in Version 4.0 of the database.

The differential elastic-scattering cross sections (DCSs) were calculated using the relativistic Dirac partial-wave method, as described by Walker [3]. The scattering potential was obtained from the self-consistent Dirac-Hartree-Fock electron density for free atoms [4] with the local exchange potential of Furness and McCarthy [5]. The numerical calculations were performed with the algorithm described by Salvat and Mayol [6]. Transport cross sections were calculated from the DCSs as described by Jablonski *et al.* [1].

2. Operation of the Database

Version 4.0 of the database has been designed to make operation of the database as easy and intuitive as possible. Help information is available on many of the screens.

Figure 1 shows the upper portion of the introductory screen. A user can click on one of the first two main menu options in the upper part of this screen, **Elastic-Scattering Cross Sections** or **Transport Cross Sections**, to go directly to screens that will provide the desired data after selection of an element from the Periodic Table, as described in Sections 2.1 or 2.2, respectively. Alternatively, a user can choose to click on the third main menu option, **Search**, or on the **Access the Database** button to enter the symbol for an element and then select the desired data, as described in Sections 2.3 and 2.4, respectively. The **More Options** button will be described in Section 2.5.
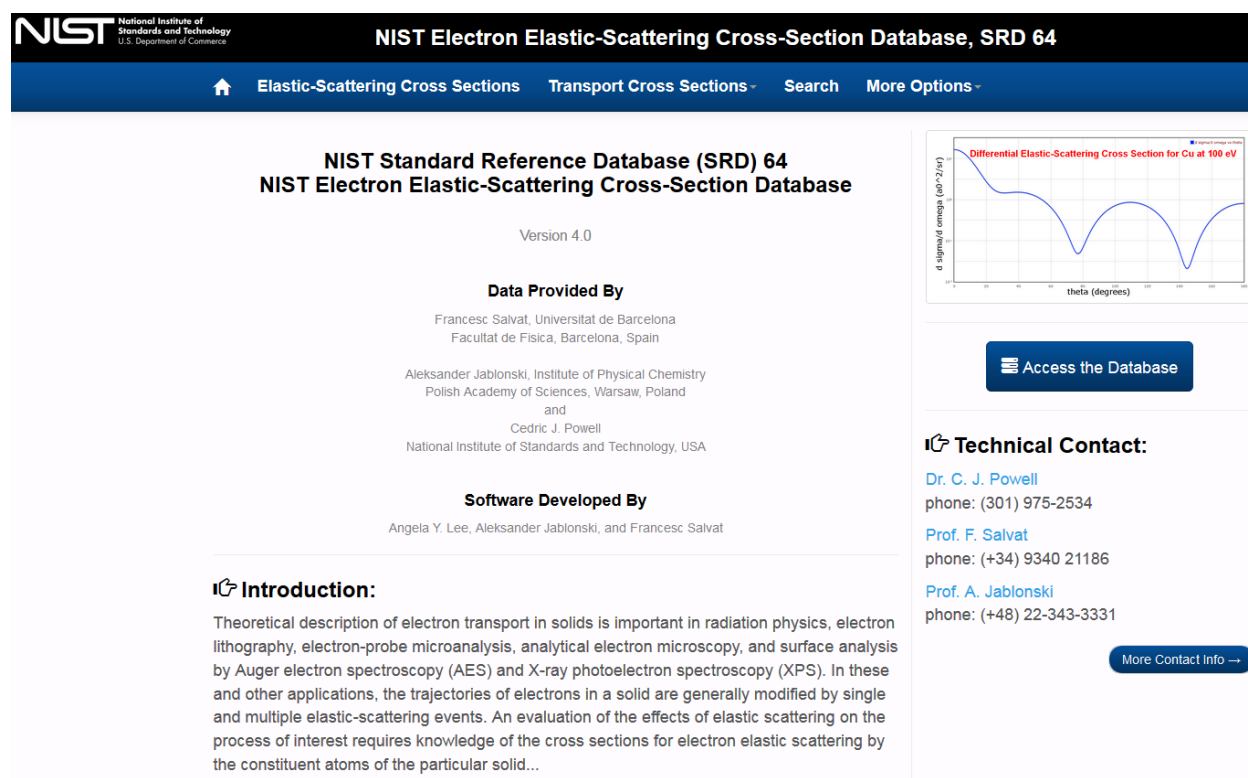
Fig. 1. Upper portion of the introductory screen.

2.1 Elastic-Scattering Cross Sections

After clicking on **Elastic-Scattering Cross Sections**, the first main menu option on the introductory screen, a Periodic Table of the elements will appear, as shown in Fig. 2. The user will then click on the symbol of the desired element and the screen of Fig. 3 will appear. For the example screen of Fig. 3, Au has been chosen together with an electron energy of 50 eV.

3

Fig. 2. Screen for selecting an element.

Fig. 3. Screen for selecting electron energy and coordinates.

A selection then needs to be made in the screen of Fig. 3 of the coordinates for display of the differential elastic-scattering cross section. Three coordinate systems are available for electron energies of 20 keV and below in which the differential elastic-scattering cross section is expressed with respect to solid angle Ω, polar scattering angle θ, or $\sin(\theta/2)$:

(a) $d\sigma / d\Omega$ *versus* θ

(b) $d\sigma / d\theta$ *versus* θ

(c) $d\sigma / d\sin(\theta/2)$ *versus* $\sin(\theta/2)$

In the latter case, the cross section $d\sigma / d\sin(\theta/2)$ is related to the differential cross section for electron momentum change $d\sigma / dq$. The quantity q is defined by $q = \left| \mathbf{K'} \text{-} \mathbf{K} \right|$ where $\mathbf{K}$ and $\mathbf{K'}$ are wave vectors before and after an elastic collision. We have:

$$\frac{d\sigma}{d\sin(\theta/2)} = 2K\frac{d\sigma}{dq}$$

where $K = |\mathbf{K}|$. For electron energies of 20 001 eV and above, cross sections are available only in $d\sigma/d\Omega$ *versus* θ coordinates.

The elastic-scattering cross sections calculated by the database are expressed in units involving the square of the Bohr radius a_0 (the radius of the first Bohr orbit of the hydrogen atom) where $a_0 = 5.291\ 772\ 1 \times 10^{-11}$ m and $a_0^2 = 2.800\ 285\ 2 \times 10^{-21}$ m^2. The specific units for the cross sections in the different coordinate systems are as follows:

(a) a_0^2 /steradian for the $d\sigma/d\Omega$ *versus* θ coordinate system;
(b) a_0^2 /radian for the $d\sigma/d\theta$ *versus* θ coordinate system; and
(c) a_0^2 for the $d\sigma/d\sin(\theta/2)$ *versus* $\sin(\theta/2)$ coordinate system.

These units are used in the screen displays and in the files created by the database.
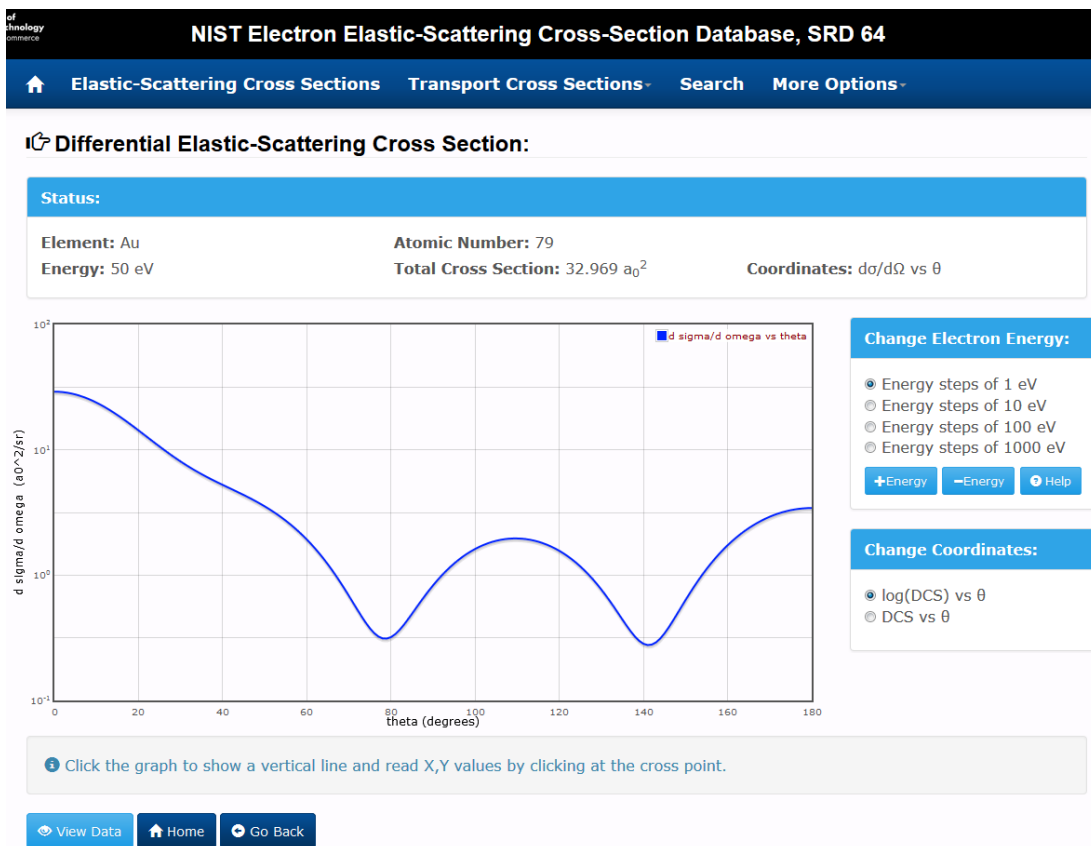
Fig. 4(a). Screen showing the differential cross section for Au in $d\sigma/d\Omega$ *versus* θ coordinates at 50 eV on semi-logarithmic scales.

5

After selection of the electron energy and the coordinate system on the screen of Fig. 3, the user will click **Display** and the screen of Fig. 4(a) will appear. For this example, the DCS for Au in the $d\sigma/d\Omega$ *versus* θ coordinate system is shown for an energy of 50 eV.

For cross sections in $d\sigma/d\Omega$ *versus* θ coordinates and for electron energies of 20 keV and below, the differential cross sections can be displayed on logarithmic or linear scales versus polar scattering angle on a linear scale. For Fig. 4(a), the DCS is displayed on a semi-logarithmic scale while the DCS on a linear scale is shown in Fig. 4(b).

Fig. 4(b). Screen showing the differential cross section for Au in $d\sigma/d\Omega$ *versus* θ coordinates at 50 eV on linear scales.

The initially selected energy can be changed by clicking the + **energy** or - **energy** buttons; these changes will occur in steps of 1 eV, 10 eV, 100 eV, or 1000 eV (within the range 50 eV to 20 keV). The total cross section for the selected energy is given above the plot.

For electron energies of 20 001 eV and above, the differential cross sections can be displayed only sections in $d\sigma/d\Omega$ *versus* θ coordinates. Displays can be shown on logarithmic scales, as shown in Fig. 5(a), or on semi-logarithmic scales, as shown in Fig. 5(b). For these examples, the DCS for Au is shown for an energy of 50 keV. The initially selected energy can be varied in steps of 10 eV, 100 eV, 1 keV, or 10 keV.

6

Fig. 5(a). Screen showing the differential cross section for Au in $d\sigma/d\Omega$ *versus* θ coordinates at 50 keV on logarithmic scales.

Fig. 5(b). Screen showing the differential cross section for Au in $d\sigma/d\Omega$ *versus* θ coordinates at 50 keV on semi-logarithmic scales.
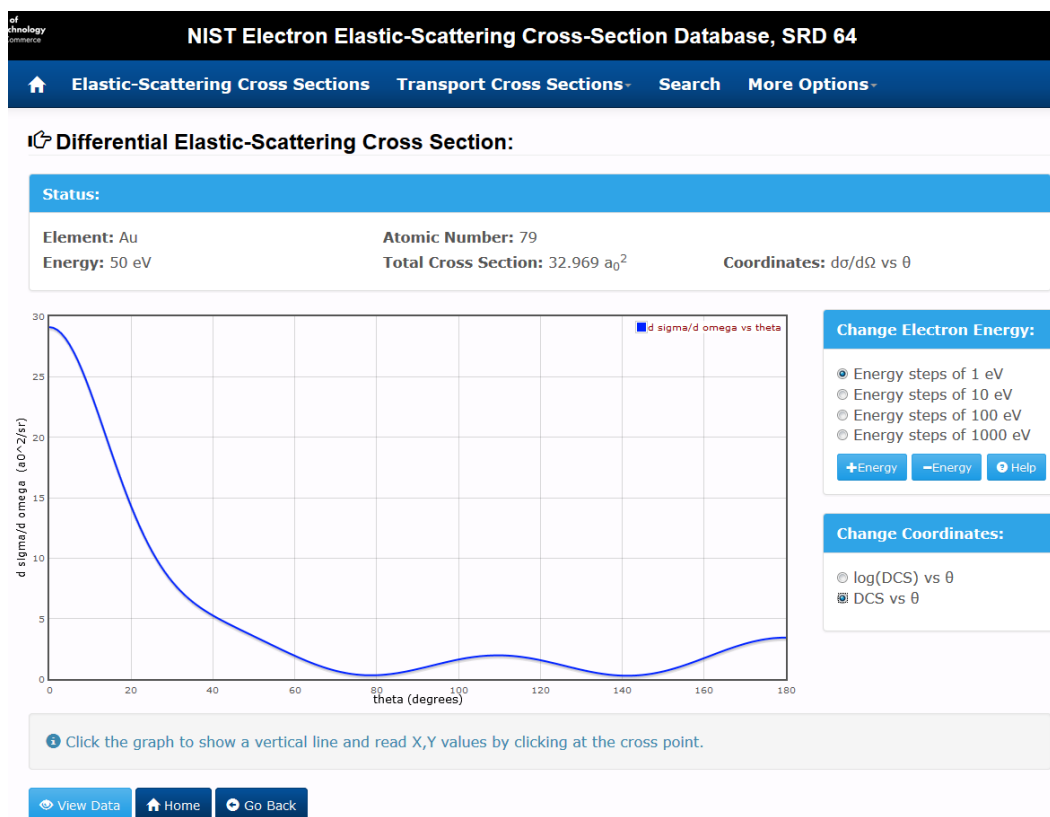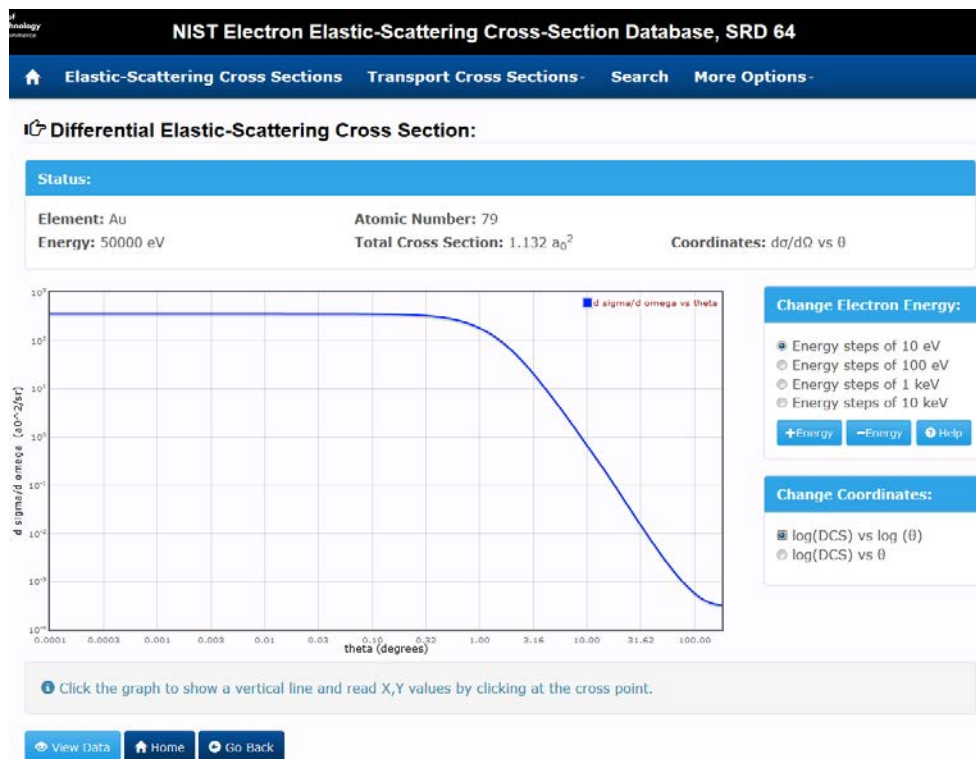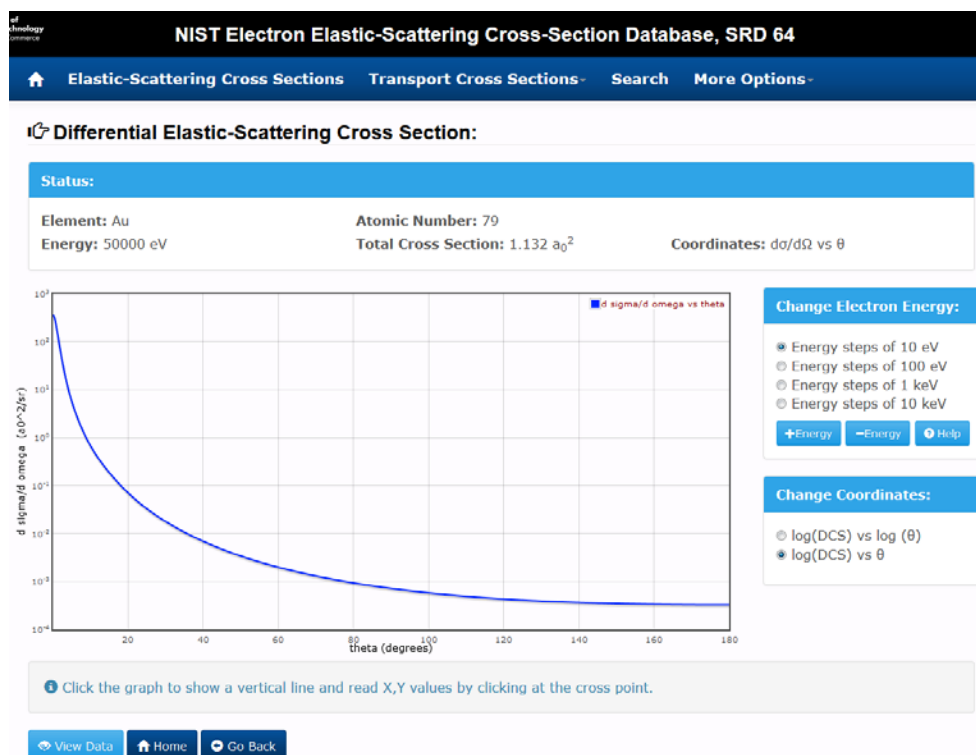
Fig. 6. Screen showing the differential cross section for Au in $d\sigma/d\theta$ *versus* θ coordinates at 50 eV on linear scales.

Fig. 7. Screen showing the differential cross section for Au in $d\sigma/d\sin(\theta/2)$ *versus* $\sin(\theta/2)$ coordinates at 50 eV on linear scales.

If the cursor is moved into the area of a graphical display, a vertical red line will appear. Clicking in the vicinity of a crossing point of this line and the graph will display the X,Y values at this point. Figures 6 and 7 show example plots of the DCS for Au at 50 eV in the $d\sigma/d\theta$ *versus* θ and $d\sigma/d\sin(\theta/2)$ *versus* $\sin(\theta/2)$ coordinate systems, respectively.

If the **View Data** button is clicked (e.g., at the bottom of the example screens in Figs. 4 to 7), a Table will appear of the numerical data used in the preparation of the particular plot. The user can choose to download the data in one of the three available formats (JSON, CSV, or text files) by clicking on the corresponding **JSON Data File**, **CSV Data File**, or **Text Data File** buttons.

2.2 Transport Cross Sections

The definition of the transport cross section is given in Section 3. If the **Transport Cross Sections** option of the main menu (Fig. 1) is chosen, a submenu of three choices appears:

(a) Display TCS (transport cross-section) values
(b) Single/multiple TCS (transport cross-section) values
(c) Table of TCS (transport cross-section) values

For each option, a screen with the Periodic Table appears (similar to Fig. 2) and the user selects an element of interest. The following screens for options (a), (b), and (c) enable TCS data for the selected element to be displayed graphically as a function of energy, allow TCS data for user-specified energies to be displayed, and enable TCS data to be displayed at regularly spaced electron energies, respectively. Files containing TCS values can be downloaded for all three options. The TCS values are shown in units of a_0^2.

For option (a), a user will first select an initial energy (between 50 eV and 300 keV), as shown in Fig. 8. In this example, Au had been previously chosen and an initial energy of 1000 eV has been selected.

Fig. 8. Screen for selecting initial electron energy.

TCS values are displayed as a function of electron energy in either of two energy ranges, 50 eV to 20 keV or 1 keV to 300 keV, depending on the user's choice of an initial energy. Example screens

9

are shown in Figs. 9(a) and 9(b) for Au with initial energies of 1000 eV and 50 keV, respectively. A value of the transport cross section for the chosen initial energy is then displayed above the plot. The selected initial energy can be changed by clicking on the **+ energy** or **- energy** buttons; these changes will occur in steps of 1 eV, 10 eV, 100 eV, or 1000 eV depending on the choice of button selected. The energy dependence of the cross section can be displayed on linear, semi-logarithmic, or logarithmic scales; these scales are chosen with the buttons in the upper-right part of the screen.
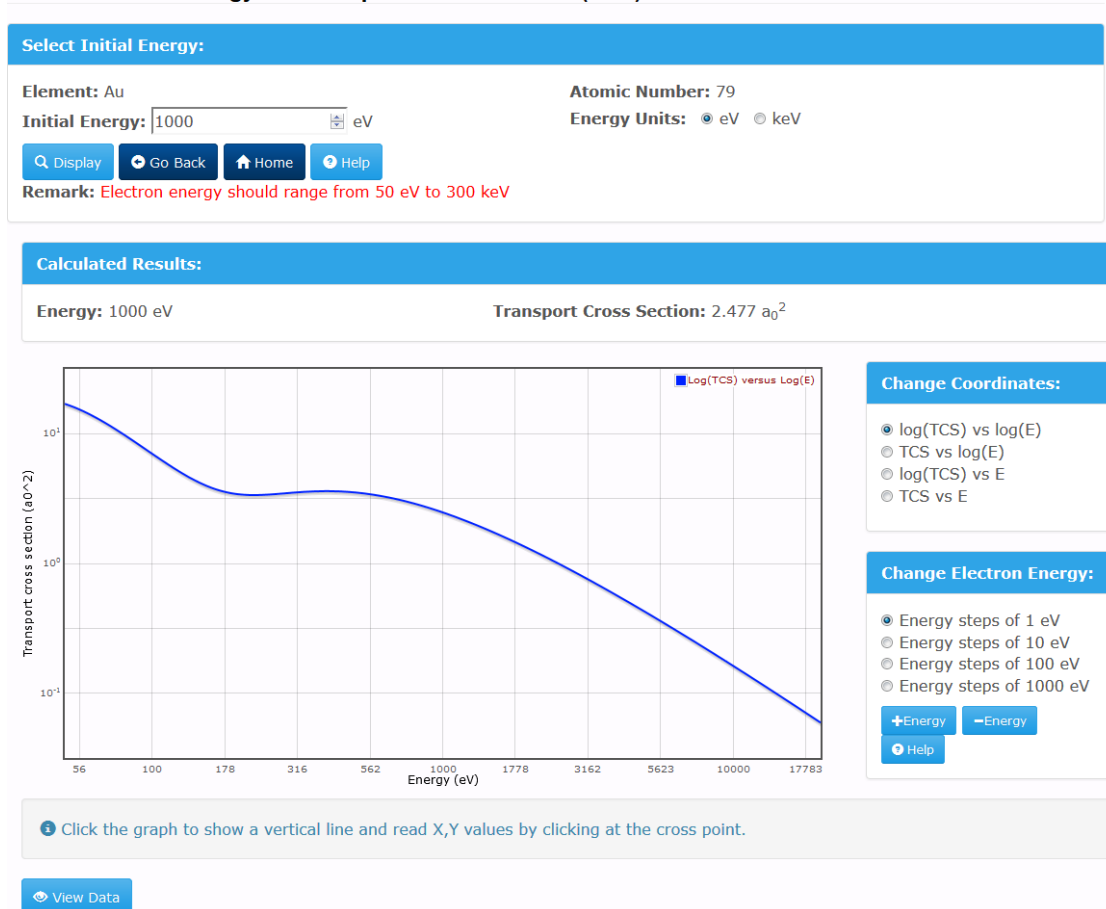
Fig. 9(a). Screen showing the energy dependence of the transport cross section for Au in the energy range from 50 eV to 20 keV.

If the cursor is moved into the area of a graphical display, a vertical red line will appear. Clicking in the vicinity of a crossing point of this line and the graph will display the X,Y values at this point.

If the **View Data** button is clicked (e.g., at the bottom of the example screens in Figs. 9(a) and 9(b)), a Table will appear of the numerical data used in the preparation of the particular plot. The user can choose to download the data in one of the three available formats (JSON, CSV, or text files) by clicking on the corresponding **JSON Data File**, **CSV Data File**, or **Text Data File** buttons.

10
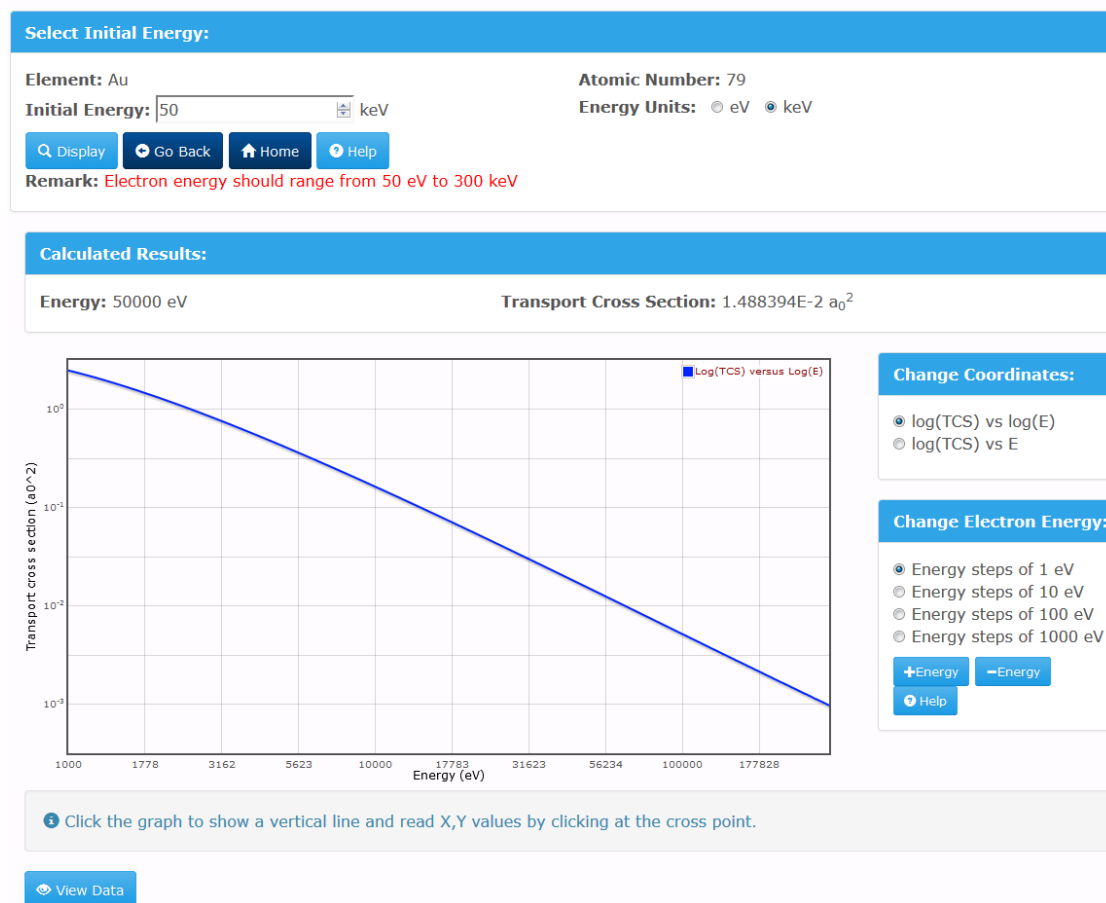
Fig. 9(b). Screen showing the energy dependence of the transport cross section for Au in the energy range from 1 keV to 300 keV.

For option (b), the user can display transport cross sections for one or more electron energies and create files with these values using the screen shown in Fig. 10 (after selection of Au for this example). The user enters the energy value of interest (between 50 eV and 300 keV) in a box. On clicking the **Add** button, the transport cross section for this energy is calculated and displayed in the box in the central part of the screen. Additional energies can be entered in the same way and the corresponding transport cross sections will be displayed in the central box. The user can then choose to download the TCS data in one of the three available file formats.

With option (c), the user can display a Table of transport cross sections at regularly spaced electron energies. The screen of Fig. 11 appears (after selection of Au for this example) and the user enters the number of transport-cross-section values desired (with a maximum of 401 values) and the minimum and maximum energies. The user also chooses whether the electron energies should be distributed linearly or logarithmically in the specified energy range by selecting one of the buttons. After clicking the **Create** button, the Table of cross section values is calculated and displayed as shown in Fig. 12. As for options (a) and (b), a user can choose to download the data in one of the three available formats (JSON, CSV, or text files) by clicking on the corresponding **JSON Data File**, **CSV Data File**, or **Text Data File** buttons.

11

👉 **Single/Multiple Transport Cross Section Values:**

Single/Multiple Transport Cross Section Values:

Element: Au   Atomic Number: 79

Energy: [100000] eV

[+ Add] [⊘ Go Back] [❓ Help]

Remark: Electron energy should range from 50 eV to 300000 eV

Single/Multiple Transport Cross Section Values:

[⬇ JSON Data File] [⬇ CSV Data File] [⬇ Text Data File]

No. ▲	Energy (eV) ⬍	TCS (a_0^2) ⬍	Action ⬍
1	50	17.016	🗑 Delete
2	100	7.008	🗑 Delete
3	200	3.409	🗑 Delete
4	500	3.526	🗑 Delete
5	1000	2.477	🗑 Delete
6	2000	1.286	🗑 Delete
7	5000	4.209763E-1	🗑 Delete
8	10000	1.624083E-1	🗑 Delete
9	20000	5.927855E-2	🗑 Delete
10	50000	1.488394E-2	🗑 Delete
11	100000	5.148827E-3	🗑 Delete

ℹ Help:

👉 **To sort desired column in the table, click on its column header.**

👉 **Three types of data files can be downloaded:**

- Javascript Object Notation (JSON) files
- Comma separated variable (csv) files that can be opened by spreadsheet software.
- Text files that can be easily read by user programs.

[⬇ JSON Data File] [⬇ CSV Data File] [⬇ Text Data File]

Fig. 10. Transport cross sections calculated for Au at selected energies.

NIST Electron Elastic-Scattering Cross-Section Database, SRD 64

🏠 **Elastic-Scattering Cross Sections**   **Transport Cross Sections**▾   **Search**   **More Options**▾

👉 **Table of Transport Cross Section Values:**

Create Table of Transport Cross Section Values:

Element: Au   Atomic Number: 79

Distribution of TCS Values: ◉ Linear Distribution   ○ Logarithmic Distribution

Number of TCS Values (Max. 401): [401]

Minimum Energy (eV): [50]

Maximum Energy (eV): [300000]

[⊕ Create] [⊘ Go Back] [🏠 Home]

Fig. 11. Screen for creating a Table of transport cross section values.

12

☞ Table of Transport Cross Section Values:

Create Table of Transport Cross Section Values:

Element: Au   **Atomic Number:** 79

Distribution of TCS Values: ⦿ Linear Distribution   ◎ Logarithmic Distribution

Number of TCS Values (Max. 401): 401

Minimum Energy (eV): 50

Maximum Energy (eV): 300000

⊕ Create   ⊕ Go Back   ⌂ Home

Table of Transport Cross Section Values:

⬇ Data File (JSON Format)   ⬇ Data File (CSV Format)   ⬇ Text Data File

No ▲	Energy (eV) ⇕	TCS (a_0^2) ⇕
1	50	17.016
2	799.88	2.892
3	1549.75	1.679
4	2299.62	1.101
5	3049.5	7.894236E-1
6	3799.38	6.007384E-1
7	4549.25	4.765433E-1
8	5299.12	3.897601E-1
9	6049	3.263318E-1
10	6798.88	2.783256E-1
11	7548.75	2.409636E-1
12	8298.62	2.112153E-1
13	9048.5	1.870756E-1
14	9798.38	1.671703E-1
15	10548.25	1.505299E-1

ℹ Help:

☜ **To sort desired column in the table, click on its column header.**

☜ **Three types of data files can be downloaded:**

- Javascript Object Notation (JSON) files
- Comma separated variable (csv) files that can be opened by spreadsheet software.
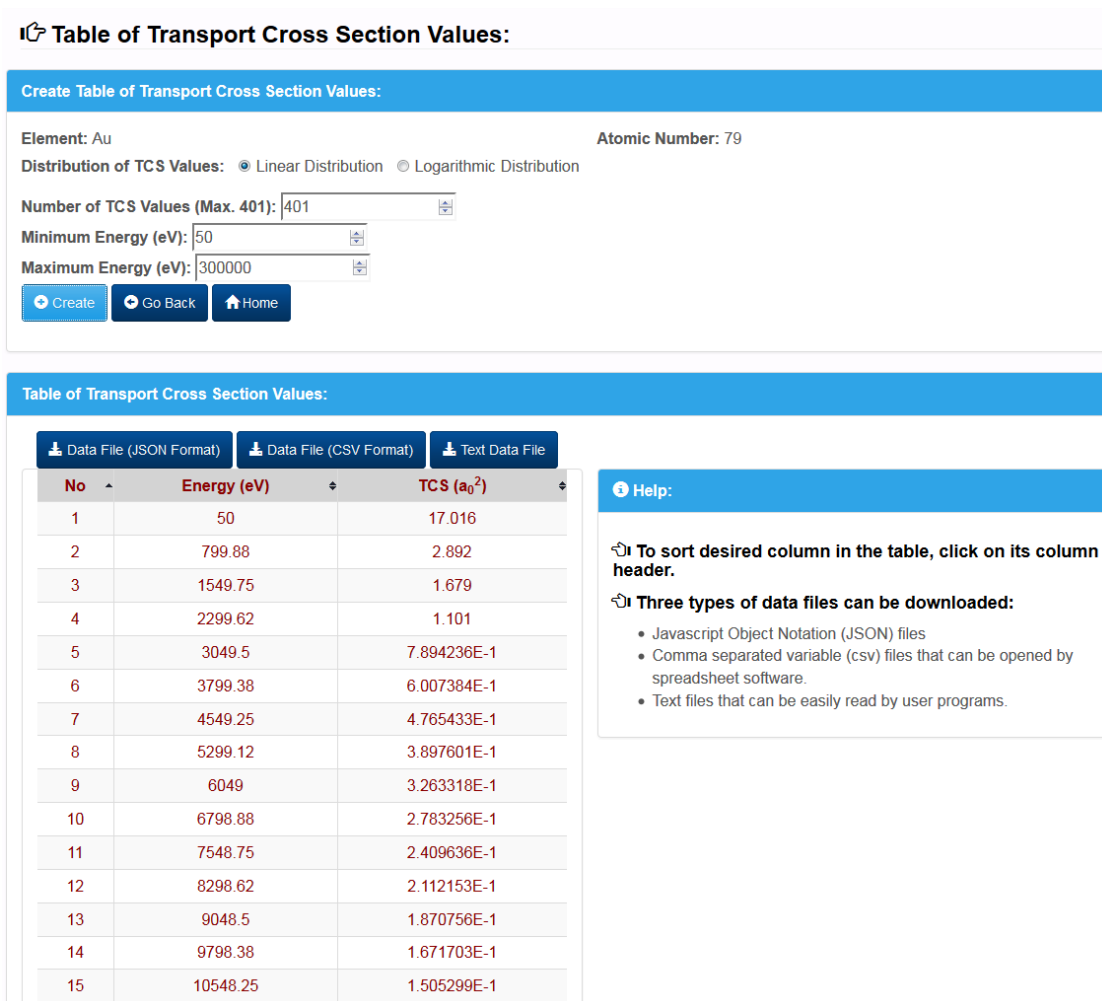- Text files that can be easily read by user programs.

Fig. 12. Screen showing part of a Table of transport cross sections for Au at the indicated energies.

2.3 Search Option

Clicking the **Search** option on the main menu brings the screen shown in Fig. 13(a) which allows a user to enter an elemental symbol in the box. After clicking the Search button on this screen, the screen shown in Fig. 13(b) appears. The user can then click on the appropriate link to obtain elastic-scattering cross sections or transport cross sections (with the options of displaying TCS values, obtaining single or multiple TCS values at user-specified energies, or creating a Table of TCS values, as described in Section 2.2).

2.4 Access the Database button

The **Access the Database** option on the introductory screen (Fig. 1) provides the same functions as the **Search** option on the main menu (Section 2.3).

13

Fig. 13(a). Screen for selection of an element from the **Search** option.

Fig. 13(b). Screen showing options for obtaining differential and total elastic-scattering cross sections and for obtaining transport cross sections from the **Search** option.

2.5 More Options

The **More Options** button on the introductory screen (Fig. 1) allows the user to access the following information:

- **About** (with basic information on the database and two references [1,2] that discuss evaluation of the data, methods of determination, and uncertainty)
- **Introduction** (with the text given on the introductory screen)
- **Acknowledgments**
- **Version History**
- **Disclaimers**
- **Citation Guide**
- **Contact Information**

14

3. Theory

3.1 Differential Cross Sections for Elastic Scattering

The differential cross sections (DCSs) for elastic scattering were calculated using the relativistic Dirac partial-wave analysis, as described by Walker [3]. The scattering potential was obtained from the self-consistent Dirac-Hartree-Fock (DHF) density for free atoms [4] with the local exchange potential of Furness and McCarthy [5]. The numerical calculations were performed with the algorithm described by Salvat and Mayol [6]. Further details are given elsewhere [1,2].

The DCS is related to the phase shifts, $\delta_l^\pm$, of order l by the following expressions [3]:

$$d\sigma_e / d\Omega = \left| f(\theta) \right|^2 + \left| g(\theta) \right|^2, \tag{1}$$

where $f(\theta)$ and $g(\theta)$ are the direct and indirect scattering amplitudes, respectively, given by:

$$f(\theta) = \frac{1}{2iK} \sum_l \left\{ (l+1)[\exp(2i\delta_l^+) - 1] + l[\exp(2i\delta_l^-) - 1] \right\} P_l(\cos\theta) \tag{2}$$

$$g(\theta) = \frac{1}{2iK} \sum_l [\exp(2i\delta_l^-) - \exp(2i\delta_l^+)] P_l^1(\cos\theta). \tag{3}$$

In Eqs. (2) and (3), $P_l(\theta)$ are Legendre polynomials, and $P_l^1(\theta)$ are associated Legendre polynomials:

$$P_l^1(z) = (1 - z^2)^{1/2} \frac{dP_l(z)}{dz}.$$

The phase shifts $\delta_l^\pm$ are obtained from the large-r behavior of the radial wave functions, $P_l^\pm(r)$ and $Q_l^\pm(r)$ which are calculated by integrating the radial Dirac equations:

$$\frac{dP_l^\pm}{dr} = -\frac{k^\pm}{r} P_l^\pm(r) + \frac{E - V + 2mc^2}{c\hbar} Q_l^\pm(r) \tag{4a}$$

$$\frac{dQ_l^\pm}{dr} = -\frac{E - V}{c\hbar} P_l^\pm(r) + \frac{k^\pm}{r} Q_l^\pm(r), \tag{4b}$$

where E is the kinetic energy of the projectile electron that is related to its total energy W by $E = W - mc^2$, $V(r)$ is the interaction potential as a function of radius r, m is the electron rest mass, and c is the velocity of light. The solution algorithm implements Bühring's power-series method [7] and is based on a cubic-spline interpolation of the potential function $rV(r)$ which is tabulated on a dense grid of r values,

15

$$r_1 = 0 < r_2 \cdots < r_{N-1} < r_N. \tag{5}$$

That is, between each pair of consecutive grid points, r_n and r_{n+1}, the potential function, $rV(r)$, is represented as a piecewise cubic polynomial in r:

$$rV(r) = a_n + b_n r + c_n r^2 + d_n r^3. \tag{6}$$

Then, in the interval (r_n, r_{n+1}), the radial functions can be formally expressed by power series:

$$P_l^\pm(r) = r^\alpha \sum_{i=0}^\infty p_i r^i \qquad Q_l^\pm(r) = r^\beta \sum_{i=0}^\infty q_i r^i, \tag{7}$$

with coefficients determined by the values of $P_l^\pm(r_n)$ and $Q_l^\pm(r_n)$ at the end point of the interval. As these series expansions can be summed up to the required accuracy (9 significant digits in the code), truncation errors are practically avoided.

The interaction potential $V(r)$ is defined as:

$$V(r) = -e\varphi(r) + V_{exc}(r), \tag{8}$$

where $\varphi(r)$ is the electrostatic potential of the target atom:

$$\varphi(r) = \frac{Ze}{r} - e\left(\frac{1}{r}\int_0^r \rho(r')\, 4\pi r'^2\, dr' + \int_r^\infty \rho(r')\, 4\pi r'\, dr' \right), \tag{9}$$

and where $\rho(r)$ is the atomic electron density that was calculated using the self-consistent DHF code of Desclaux [4].

The term $V_{exc}(r)$ in Eq. (8) is a local approximation to the exchange interaction between the projectile and the electron in the target; it should not be confused with the exchange interaction considered in self-consistent calculations that accounts for exchange between atomic electrons. We use the exchange potential of Furness and McCarthy [5]:

$$V_{exc}(r) = \frac{1}{2}[E + e\varphi(r)] - \frac{1}{2}\left\{ [E + e\varphi(r)]^2 + 4\pi \frac{\hbar^2 e^2}{m}\rho(r) \right\}^2. \tag{10}$$

The interaction potential [Eq. (8)] is thus completely determined by the atomic density $\rho(r)$.

16

The integration of the radial equations is started from $r = 0$, with boundary values:

$$P_l^{\pm}(0) = 0, \qquad\qquad Q_l^{\pm}(0) = 0. \qquad\qquad (11)$$

In the first r-interval from $r_1 = 0$ to r_2 [Eq. (5)], the constants α and β [Eq. (7)] are different from zero and determined by the angular momentum quantum numbers [8]. For the outer intervals ($r > r_2$), $\alpha = \beta = 0$.

After determining the values of the radial functions at r_2, the solution is extended outwards by using the series expansions [Eq. (7)] (with $\alpha = \beta = 0$) up to a certain radial distance r_{max}, large enough to ensure that the potential energy of the electron $V(r)$ is negligible as compared to its kinetic energy E. For selected elements and at an energy of 10 keV, the maximum ranges, r_{max}, were as follows (in a_0 units):

$$\begin{array}{lll}
\text{for } Z = 1 & r_{max} & = 12.27 \\
\text{for } Z = 13 & r_{max} & = 20.15 \\
\text{for } Z = 28 & r_{max} & = 17.85 \\
\text{for } Z = 47 & r_{max} & = 19.37 \\
\text{for } Z = 79 & r_{max} & = 17.11 \\
\text{for } Z = 96 & r_{max} & = 21.54 \\
\end{array}$$

At an energy of 20 000 eV:

$$\begin{array}{lll}
\text{for } Z = 1 & r_{max} & = 11.96 \\
\text{for } Z = 13 & r_{max} & = 19.75 \\
\text{for } Z = 28 & r_{max} & = 17.48 \\
\text{for } Z = 47 & r_{max} & = 18.80 \\
\text{for } Z = 79 & r_{max} & = 16.74 \\
\text{for } Z = 96 & r_{max} & = 21.13 \\
\end{array}$$

At sufficiently large distances r, the radial function $P_l^{\pm}(r)$ adopts the asymptotic form:

$$P_l^{\pm}(r) \cong \sin(Kr - l\frac{\pi}{2} + \delta_l^{\pm}), \qquad\qquad (12)$$

where

$$\hbar K = \frac{1}{c}\sqrt{E(E + 2mc^2)} \qquad\qquad (13)$$

17

is the momentum of the projectile. Equation (12), which confers a geometrical meaning to the phase shift, is not directly usable to compute $\delta_l^{\pm}$ because $P_l^{\pm}(r)$ reaches the form given by Eq. (12) only at distances r that may be much larger than r_{max}. Instead, the phase shift is obtained from the calculated values of the radial functions at r_{max} by matching the numerical solution to the exact solution for $r > r_{max}$ $(V = 0)$ which can be expressed as a linear combination of spherical Bessel functions, $j_k(Kr)$ and $n_k(Kr)$ of indices $k = l, l \pm 1$ [8].

A considerable number of phase shifts was found to be necessary to achieve 8-digit accuracy in the calculation of DCSs from Eqs. (1) to (3). At an energy of 10 000 eV, we have:

$$
\begin{array}{ll}
\text{for } Z = 1 & 0 \le l \le 221 \\
\text{for } Z = 13 & 0 \le l \le 386 \\
\text{for } Z = 28 & 0 \le l \le 343 \\
\text{for } Z = 47 & 0 \le l \le 369 \\
\text{for } Z = 79 & 0 \le l \le 325 \\
\text{for } Z = 96 & 0 \le l \le 422
\end{array}
$$

At an energy of 20 000 eV:

$$
\begin{array}{ll}
\text{for } Z = 1 & 0 \le l \le 307 \\
\text{for } Z = 13 & 0 \le l \le 538 \\
\text{for } Z = 28 & 0 \le l \le 478 \\
\text{for } Z = 47 & 0 \le l \le 514 \\
\text{for } Z = 79 & 0 \le l \le 452 \\
\text{for } Z = 96 & 0 \le l \le 589
\end{array}
$$

The only special functions used in calculations of the DCSs for the DHF potential are spherical Bessel functions $j_l(x)$ and $n_l(x)$. The algorithm used to compute these functions combines several analytical expressions and recurrence relations, and yields results that are accurate to 13 or more significant digits. The code used for these calculations was tested for $0 \le l \le 20\,000$ and $0 < x < 20\,000$.

3.2 Transport Cross Sections

Transport cross sections are needed for determination of numerous parameters related to electron transport in solids (the depth distribution function, the effective attenuation length, the electron mean escape depth, etc.) [9, 10]. The transport cross section describes the mean fractional momentum loss due to elastic scattering alone. We denote by **k** the electron momentum before elastic scattering, and by **k′**, the projection of the momentum after elastic scattering on the initial direction. Obviously, $\mathbf{k'} = \mathbf{k}\cos\theta$. We further denote the fractional momentum loss, due to elastic scattering alone, by

$$\Delta k = \frac{|\mathbf{k} - \mathbf{k'}|}{|\mathbf{k}|} \, .$$

The transport cross section is the product of the mean fractional momentum loss and the total elastic-scattering cross section:

$$\sigma_{tr} = \sigma_{el} \langle \Delta k \rangle = \sigma_{el} \frac{\int\limits_{4\pi} \Delta k \, (d\sigma/d\Omega) \, d\Omega}{\int\limits_{4\pi} (d\sigma/d\Omega) \, d\Omega} \, . \tag{14}$$

Equation (14) can be transformed to:

$$\sigma_{tr} = 2\pi \int\limits_0^\pi (1 - \cos\theta)(d\sigma/d\Omega) \sin\theta \, d\theta \, . \tag{15}$$

A change of the atomic potential leads to pronounced variation of the differential elastic-scattering cross section for small scattering angles and rather small variations for larger scattering angles [10]. In the integrand of Eq. (15), we have two functions approaching zero for small scattering angles: $\sin\theta$ and $(1 - \cos\theta)$. Consequently, we may expect that the sensitivity of the transport cross section to the interaction potential is much smaller than the sensitivity of the total elastic-scattering cross section. It has been shown that the transport cross sections values depend very weakly on the potential for elements with a wide range of atomic numbers (Be to Au) and for electron energies from 100 eV to 10 000 eV [11].

19

4. References

[1]   A. Jablonski, F. Salvat, and C. J. Powell, J. Phys. Chem. Ref. Data 33, 409 (2004).

[2]   F. Salvat, A. Jablonski, and C. J. Powell, Computer Physics Communications 1*65*, 1571 (2005).

[3]   D. W. Walker, Advances in Physics 20, 257 (1971).

[4]   J. P. Desclaux, Computer Physics Communications 9, 31 (1975); erratum ibid 13, 71 (1977).

[5]   J. B. Furness and I. E. McCarthy, J. Phys. B: At. Mol. Phys. 6, 2280 (1973).

[6]   F. Salvat and R. Mayol, Computer Physics Communications 74, 358 (1993).

[7]   W. Bühring, Z. Phys. **187**, 180 (1965).

[8]   F. Salvat and R. Mayol, Comput. Phys. Comm. **62**, 65 (1991).

[9]   A. Jablonski and C. J. Powell, J. Electron Spectrosc. Relat. Phenom. **100**, 137 (1999).

[10] A. Jablonski and C. J. Powell, Surf. Science Reports **47**, 33 (2002).

[11] A. Jablonski and C. J. Powell, Surf. Science **463**, 29 (2000).